DEFINITION OF THE CENTRELINE REFERENCE AIRCRAFT AND POWER PLANT SYSTEMS

F. Peter, A. Habermann, M. Lüdemann, K. Plötner, F. Troeltsch and A. Seitz
Bauhaus Luftfahrt e. V.
Willy-Messerschmitt-Straße 1, 82024 Taufkirchen, Deutschland

Julian Bijewitz
MTU Aero Engines AG
Dachauer Str. 665, 80995 München

Abstract

Within the ConcEpt validatioN sTudy foR fusElage wake-filLIng propulsioN integration (CENTRELINE) project, the proof of concept of the Propulsive Fuselage Concept (PFC) with an Entry Into Service (EIS) year of 2035 was demonstrated. The content of this paper describes the activities in Task 1.1 "Application scenario and reference aircraft" as part of the first work package in the European Union Horizon 2020 project CENTRELINE [1]. In order to assess the PFC under realistic design and operational conditions, a well-suited application scenario was required. For the PFC, environmental benchmarking against the targets defined by the European Strategic Research and Innovation Agenda (SRIA) [2], a sound baseline representing typical year 2000 standards was necessary. An analysis of the air traffic demands and aircraft (A/C) market segment trends for a target propulsive fuselage A/C entering the market in the year 2035 is presented, showing the market forecast and a very strong influence of the intercontinental traffic between Europe and Asia. Broad potential for an application in 2035 was identified for a design mission with 340 passengers and 6500 NM range. A suitable set of Top-Level Aircraft Requirements (TLAR) was compiled, based on an existing A/C design with the best possible data availability and similarity concerning the design mission requirements. This A/C was determined to be the Airbus A330-300 equipped with Rolls-Royce Trent 700 series power plants. For a fair comparison, an appropriate model of the A330-300 was deduced in order to match the 2035 design mission. The resulting configuration represents a suitable year 2000 reference (R2000), including a propulsion system appropriate for SRIA benchmarking purposes. The year 2035 reference A/C (R2035) was derived from the R2000 by incorporation of advanced conventional technologies. Family concept considerations were taken into account, and a shrink, baseline, and stretch version of the R2000 and R2035 were designed. The members of each family share common components. An advanced propulsion system featuring geared turbofan engines with ultra-high bypass ratio greater than 16 together with advanced component technologies was created for the R2035. In results, the R2035 baseline design has a block fuel reduction for the design mission of 33% compared to the R2000 baseline A/C.

Keywords

CENTRELINE, Aircraft Design, Reference Aircraft, Technology Scenario, Propulsion System

Abbreviations

A/C	Aircraft	MLA	Maneuver Load Alleviation
AC AaMP	Aircraft Characteristics – Airport and Maintenance Planning	MTOM	Maximum Take off Mass
ACI	Airports Council International	NLF	Natural Laminar Flow
AFS	Active Flutter Suppression	PFC	Propulsive Fuselage Concept
APSS	Aircraft Propulsion System Simulation	PPS	Power Plant Systems
BHL	Bauhaus Luftfahrt e. V.	RPK	Revenue Passenger Kilometers

doi: 10.25967/530114

BMI	Body Mass Index	SRIA	Strategic Research and Innovation Agenda
CFRP	Carbon Fiber Reinforced Polymer	TLAR	Top-Level Aircraft Requirements
EIS	Entry Into Service	UHBR	Ultra-High Bypass Ratio
GLA	Gust Load Alleviation	ULD	Unit Load Devices
ICAO	International Civil Aviation Organization		

1. INTRODUCTION

Within the CENTRELINE project, the proof of concept for a ground-breaking approach to synergistic propulsion-airframe integration was demonstrated, the so-called PFC [3]. The concept consists of a dedicated propulsive device that entrains and re-energizes the fuselage boundary layer flow in order to directly compensate the viscous drag effects in the fuselage wakefield. In order to assess the potential of such a concept under realistic design and operational conditions, a well-suited application scenario was required. For the PFC, environmental benchmarking against the targets defined by the European SRIA [2], a sound baseline representing typical year 2000 standards was necessary. Therefore, the first task in the CENTRELINE project was dedicated to the definition of realistic reference A/C and propulsion systems for the year 2000, the SRIA baseline A/C R2000, as well as an advanced conventional reference based on an evolutionary development of systems design paradigms, the CENTRELINE reference A/C R2035. As an enabler for this, a realistically advanced technology scenario for the R2035 A/C was developed. Both reference A/C are key parts of the CENTRELINE technology assessment process. As visualized in Figure 1, the R2035 was derived from the R2000 by introducing advanced conventional technologies. The PFC A/C results from the R2035 design by the introduction of the propulsive fuselage technology. The PFC technology evaluation was performed against the R2035, while the PFC SRIA benchmarking was conducted versus the R2000.

This paper describes the specification of the TLAR together with relevant sizing and performance characteristics of the R2000 and R2035 A/C families and Power Plant Systems (PPS). Based on market outlook perspectives, anticipated socio-economic development trends, and required transport capacities, the most suitable air transport market segment was derived for the PFC application in order to produce the most significant impact on overall air transport cumulative fuel consumption. For the targeted utilization spectrum, the most appropriate cabin capacity and A/C design range was identified, and, both A/C R2000 and R2035 were defined with a strategy for a product design family allowing for margin of future potential stretch and shrink derivatives of the baseline A/C.

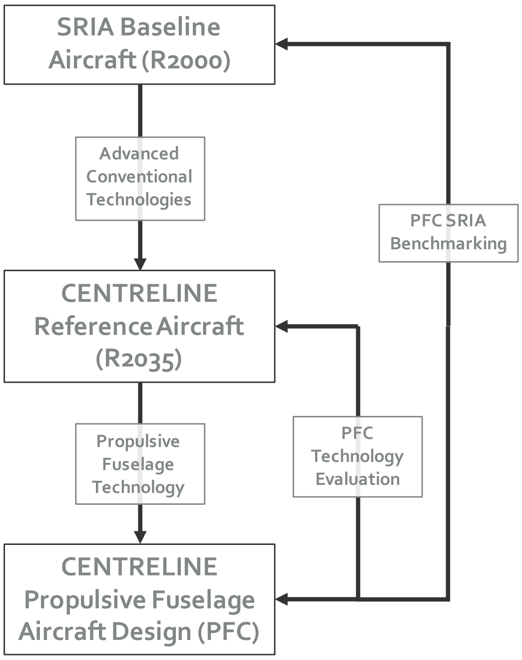

Figure 1: The CENTRELINE technology assessment process [1]

2. REFERENCE APPLICATION SCENARIO

The aviation industry has grown strongly over the past decades at a global rate of around 5% per year [4] and above, measured in transport capacity (Revenue Passenger Kilometers, RPK). During the CENTRELINE predecessor EU project DisPURSAL [5], a forecast analysis for market developments issued by all main aviation stakeholders (see Figure 2, [6–13]) was conducted, predicting further growth in transport capacity by 4 to 5 % annually until 2030 at global average. This approximately translates into doubling of transport capacity by 2030 compared to today. Particularly high growth rates, partly surpassing 6% per year, are expected for emerging countries, for example, in the Asia-Pacific region, driven by the transition to middle- or even high-income countries with a growing middle class and the associated changes in travel behavior [14].

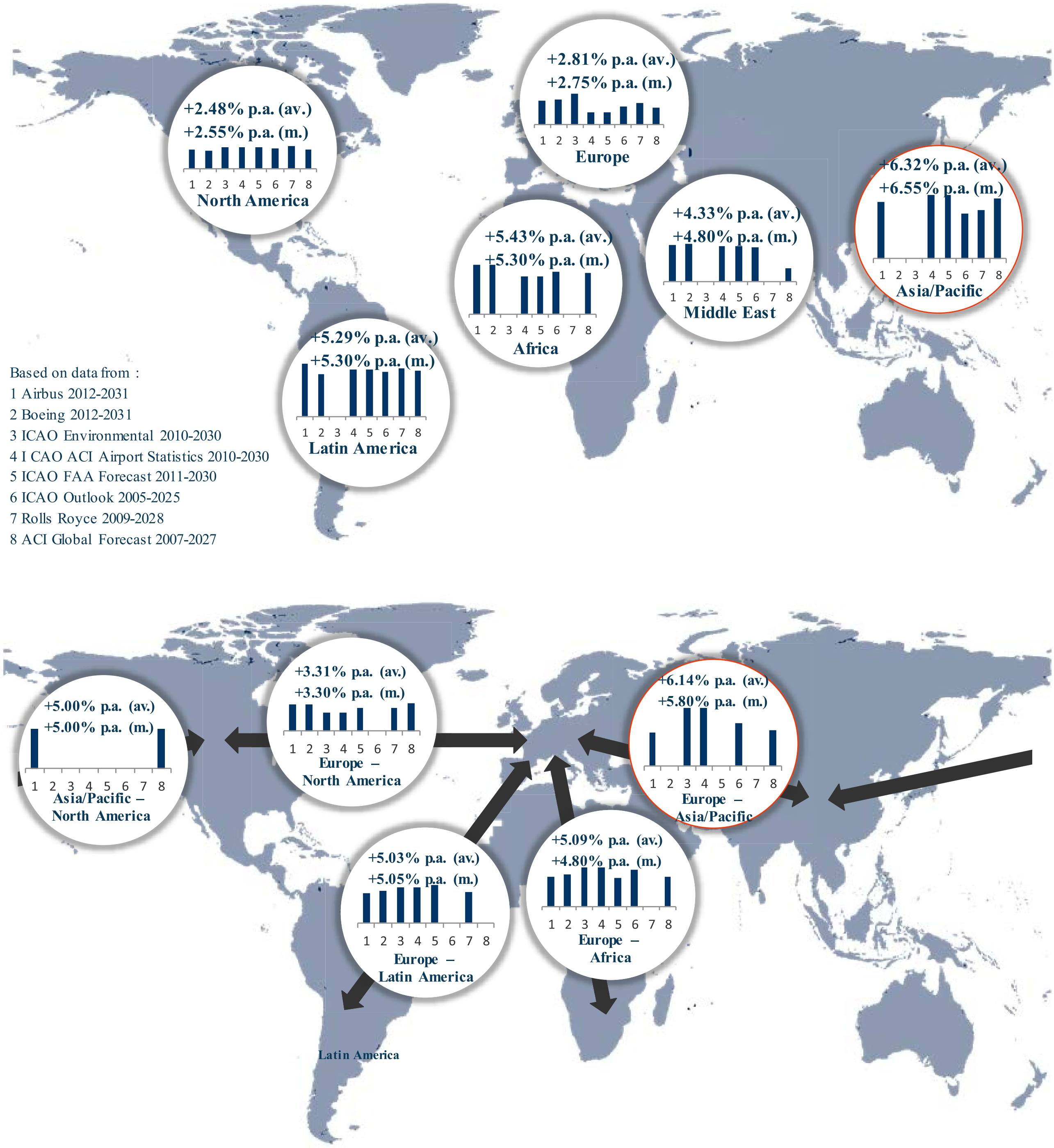

Figure 2: Annual revenue passenger kilometer growth per region and inter-region [15]

For CENTRELINE, the average RPK growth rates per region and inter-regions between 2012 and 2035 were translated into a growth of frequency (flight movements), growth in seat load factor and growth in average installed seats per A/C based on International Civil Aviation Organization (ICAO) and Airports Council International (ACI) reports. The last five years (2030-2035) were extrapolated due to the unavailability of data during the duration of DisPURSAL. However, taking recent forecasts from Airbus [16], Boing [17], and the United Aircraft Corporation [18] into account, no significant change in growth rates could be observed. The focus was defined to be on the medium-to-long haul segment above 3000 NM with more than 280 seats. Around 42% of the worldwide fuel burn accounts for this market segment. The growth rates of frequency and number of installed seats per A/C and region were applied on scheduled flight data [19]. The results for 2012 and 2035 yielded that the peak in 2012 of 301-320 seats per A/C in a typical three-class cabin configuration will shift to 321-340 seats. For CENTRELINE, a high operational flexibility approach was chosen, and the most suitable design range was found at 6500 NM, to cover 100% of all possible city pairs for A/C in the seat capacity regime of 321-340 passengers. The design range is comparable to an Airbus A330-300 today (see Figure 3).

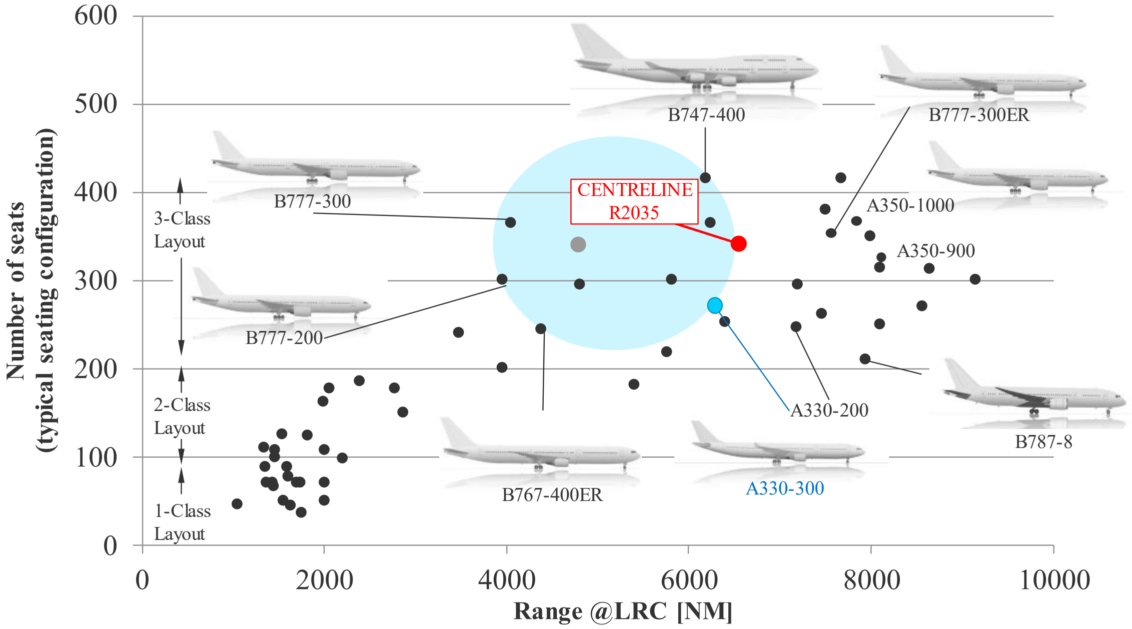

Figure 3: Number of seats and range at long-range cruise condition for various aircraft types compared to various existing aircraft types

3. DESCRIPTION OF THE R2000 SRIA AIRCRAFT FAMILY

This section describes the R2000 SRIA Baseline A/C, including the propulsion system. After a characterization of the wing and fuselage design, the modeled power plants based on a TRENT 700 are introduced, and the overall A/C design and mission performance are outlined.

3.1. R2000 Airframe

Top-Level Aircraft Requirements

In the following, the derivation of the R2000 SRIA baseline A/C from publicly available data is described. The Airbus A330-300 is identified as an A/C that is similar with respect to the transportation task determined for the R2035 A/C in Section 2. Hence, the R2000 TLAR are oriented towards the A330-300 TLAR and are listed in Table 1.

Table 1: Top-Level Aircraft Requirements for the CENTRELINE R2000

Parameter	Value
Range and PAX	6500 NM, 340 PAX in 2-class
Take-off field length (MTOM, S-L, ISA)	≤ 2600 m
2nd Climb segment conditions	340 PAX, 95 kg per PAX, DEN, ISA+20 °C
Time-to-climb (1,500 ft to ICA, ISA+10 °C)	≤ 25 mins
Initial cruise altitude (ISA+10°C)	≥ FL 330
Design cruise Mach number	0.82
Maximum cruise altitude	FL410
Approach speed (MLW, S-L, ISA)	140 KCAS
Landing field length (MLW, ISA)	≤ 2200 m
One engine inoperative altitude (drift down)	FL170
Airport compatibility limits	ICAO Code E (52 m < x < 65 m)
Aircraft classification number (flexible,B)	67
Technology freeze – entry into service	2000

Wing

The main wing, vertical and horizontal stabilizer planform are deduced from Airbus A/C 3-view CAD drawings [20] and the "Aircraft Characteristics – Airport and Maintenance Planning" (AC-AaMP) document [21]. To reduce complexity, while keeping the aerodynamic properties similar, a simplified wing planform was developed, consisting of three segments. Thickness-to-chord ratio and twist distribution for the wing were determined by an approximation of data available for the equivalent Airbus A340-200/-300 wing span-wise thickness and twist distribution [22] (see Figure 4).

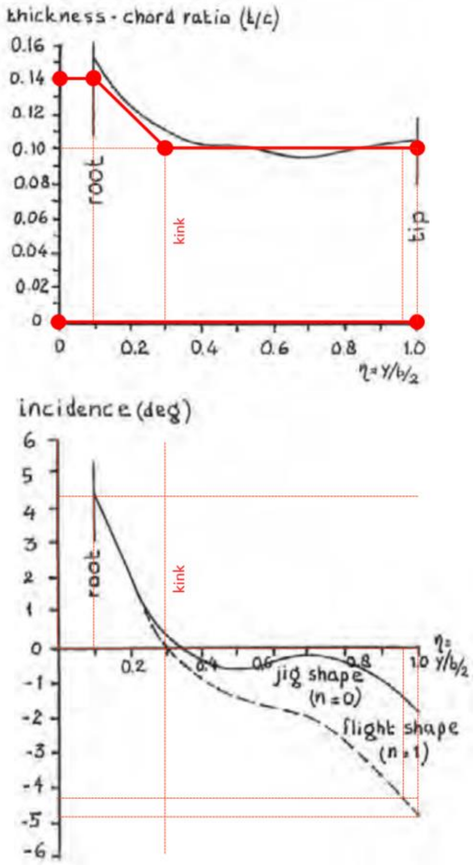

Figure 4: Airbus A340 spanwise thickness (top) and twist distribution (bottom) [22]

The airfoils were selected from the NASA supercritical airfoil family [23], with 10 % (NASA SC(2)-0710) and 14 % (NASA SC(2)-0714) thickness-to-chord ratio respectively (see Figure 5). The wing loading was defined by an optimization study for the stretch family member with economic mission block fuel as optimization target. The span limit dictated by the ICAO Code E box limit was set as a boundary.

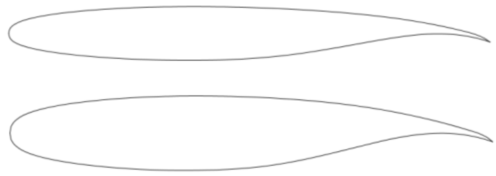

Figure 5: NASA SC(2)-0710 (top) and NASA SC(2)-0714 (bottom) supercritical airfoils [23]

The resulting wing reference area for the R2000 family is 441 m² with an aspect ratio of 9.3. For representative cruise conditions, the overall aerodynamic performance of the R2000 baseline is given in Table 2.

Table 2: R2000 baseline aerodynamics for cruise conditions (FL350, Ma = 0.82, lift coefficient = 0.5)

Parameter	Value
Zero lift drag coefficient	56.2 %
Induced drag coefficient	37.1 %
Wave drag coefficient	6.7 %
Lift to drag ratio	20.0

Fuselage

The fuselage design of the R2000 baseline was derived from the A330-300 layout, which is a two-class layout with 300 passengers [21]. The A330 design features a six-abreast configuration (2-2-2) in the business class and an eight-abreast (2-4-2) in the economy class, as illustrated in Figure 6. The passengers in the business class are seated in 21 in (0.53 m) wide seats, while the seat width was reduced to 18 in (0.48 m) in the economy class. The cargo compartment houses 36 LD3 Unit Load Devices (ULD). The outer circular fuselage diameter is 5.64 m, and the maximum cabin width is 5.28 m. The designs of the R2000 and R2035 incorporate an A/C family concept, sharing the majority of the parts: wing, horizontal stabilizer, landing gear, pylons, and propulsion system. The addition or removal of common barrel sections from the baseline fuselage created the shrink or stretch fuselage version. This common approach enabled the creation of shrink and stretch fuselage versions. The resulting fuselage dimensions are listed in Table 3.

Table 3: Fuselage dimensions of the R2000 family

Parameter	Shrink	Baseline	Stretch
Passengers [-]	296	340	375
Length [m]	61.6	67.7	73.2
Diameter [m]	5.64	5.64	5.64
Slenderness [-]	10.9	12.0	13.0

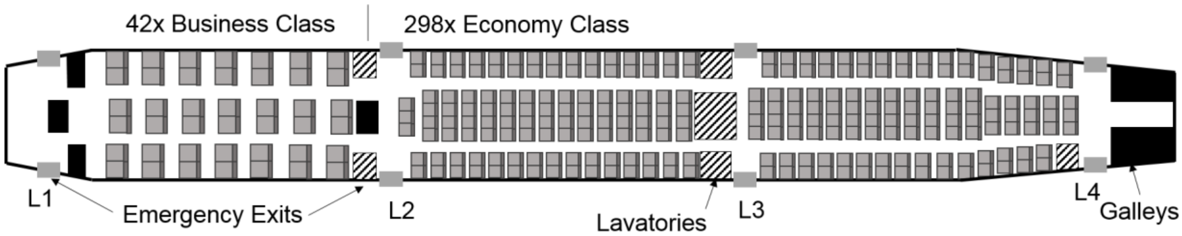

Figure 6: R2000 cabin layout

Overall Airframe

The structural concept of the R2000 is identical to the A330-300 structural setup. Main structural components are fabricated from aluminum alloy. The wing is featuring two spars along the whole wingspan and an additional spar extending to the pylon attachment. The fuselage is a fully metallic, semi-monocoque and fail-safe design consisting of skin, stringer, and milled frames. The empennage consists of a classic, fuselage-mounted vertical and horizontal tail. The vertical fin is based on three spars in the root section and two spars in the tip section. One fuel tank is located in the torsion box of the horizontal stabilizer. Both horizontal and vertical tailplanes are composed of Carbon Fiber Reinforced Polymer (CFRP) and glass fiber reinforced polymer, whereas the rudder and elevator consist of a sandwich structure using CFRP face sheets and a honeycomb core. The major structural component mases of the R2000 A/C are listed in Table 4.

Table 4: R2000 baseline mass breakdown

Component	Mass [t]
Wing	46.8
Fuselage	27.9
Vertical tailplane	2.5
Horizontal tailplane	3.1
Landing gear	12.5
Pylons	4.6
Propulsion system	23.2
Systems	10.2
Furnishing	13.2
Operational items	8.2
Operational empty mass	152.1

The R2000 baseline A/C 3-view is given in Figure 7.

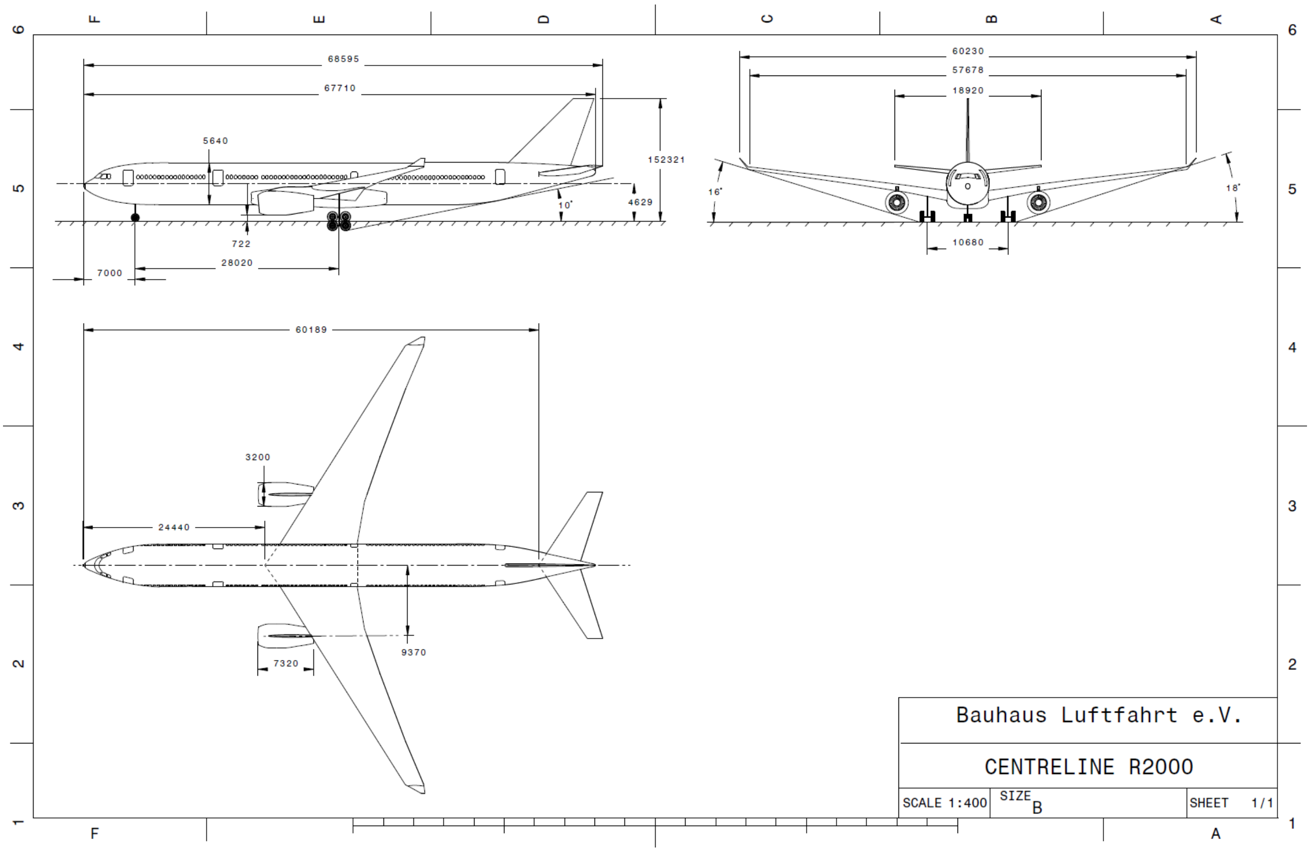

Figure 7: 3-view of the R2000 baseline, dimensions in mm

3.2. R2000 Power Plant

Due to the similar transport task and technology level of the R2000, the A/C is powered by the propulsion system of the A330-300 A/C. For this A/C, three different power plant options are available, including the GE CF6-80E1 series, the Pratt & Whitney PW4000, and the Rolls-Royce Trent 700 series. As of 2015, the by far largest market share can be attributed to the Trent 700 engine [24]. One of its latest variants, the Trent 772B, delivers 71100 lbf static thrust (316.3 kN) and is flat-rated to ISA+22 K at 2000 ft altitude [25]. The engine certification of the baseline variant was achieved in 1994 [26]. The turbofan features a three-spool architecture with a mixed-flow nacelle. The fan is driven by a four-stage low-pressure turbine, whereas the eight-stage intermediate-pressure compressor and the six-stage high-pressure compressor are powered by single-stage intermediate and high-pressure turbines, respectively. Propulsion system design and performance synthesis were conducted using the Aircraft Propulsion System Simulation (APSS) framework, which was in-house developed by BHL (Bauhaus Luftfahrt e. V.) [27–29]. APSS features a similar fidelity of component models as the commercial software GasTurb™ [30], however, it allows for a higher flexibility with regards to the simulation of uncommon engine architectures, and highly reduces the calculation time through extensive use of vectorization. Main engine data are provided in Table 5.

Table 5: Modelled Trent 772B key data

Parameter	Value
Fan diameter	2.93 m
Nacelle diameter	3.72 m
Nacelle length	8.98 m
Design bypass ratio	4.8*
Nominal take-off thrust (SLS, ISA+0 K)	409.5 kN
Thrust-specific fuel consumption mid-cruise (@FL370, Ma = 0.82, 60.5 kN)	16.5 [g/s/kN]

*Flow path sizing point at top-of-climb (Ma = 0.82, FL350, ISA+10 K)

Flow path sizing was conducted at Top-of-Climb (ToC) conditions. A multi-point sizing strategy was applied, allowing for the incorporation of the effects of maximum temperature levels, mechanical loadings, and, if applicable, fan-drive-gear-efficiency implications within the cycle design [28]. For the modeling of the R2000 power plant, information from [26], as well as data specified in the Type Certificate Data Sheets of FAA [31] and EASA [25] were used to validate the modeled design and performance characteristics. Component hub/tip ratios and other important geometric properties were graphically approximated from a 2D general arrangement given in [26]. The compressor work was adjusted to yield reasonable compressor stage loadings and mean stage pressure ratios. As part of the multi-point sizing strategy, turbo component tip speeds were iterated to yield the maximum rotational spool speeds at hot-day take-off conditions specified in [25]. The results show good agreement with the available performance data.

3.3. R2000 Baseline Mission Performance

The data presented in Sections 3.1 and 3.2 were incorporated in Pacelab APD [32], a conceptual A/C design tool. The mission simulation integrated into APD employs a detailed mission analysis, which was applied on the R2000 A/C to assess the performance on mission level. As an example, the design mission defined by a payload of 32.3 t and a range of 6500 NM yields a block fuel of 98.0 t, with a Maximum Take-Off Mass (MTOM) of 293.2 t. Several other missions were calculated, and the resulting data integrated into the payload range diagram shown in Figure 8. The payload range diagram is a key indicator for comparing the performance of A/C and therefore the official data of the A330-300 and A330-200 from the AC-AaMP [21] are shown as well in Figure 8. The gradient of the straight connecting the first and second bend in the graph is representative of the performance on the missions conducted at MTOM and at varying payloads. This section is a good metric for judging the similarity of A/C characteristics. The gradient of the three A/C is similar, which indicates a sufficient resemblance of the R2000 baseline A/C and the official performance data of the A330-300/200. Differences in the slope can be explained by the difference in wing loading. Furthermore, the ferry range can be seen in the payload range as the intersection with the horizontal axis.

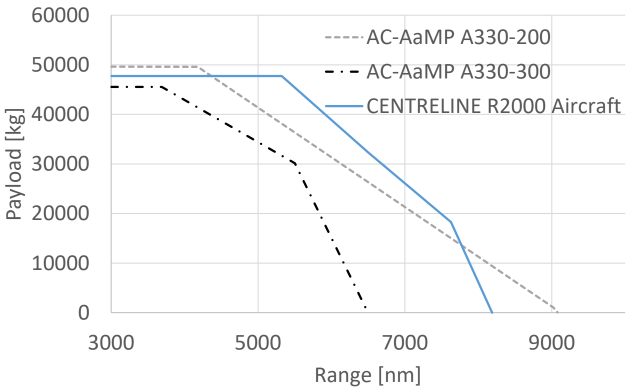

Figure 8: Payload range chart for R2000 baseline aircraft in comparison to A330-200 and A330-300 aircraft [21]

4. DESCRIPTION OF THE R2035 AIRCRAFT FAMILY

Similar to Section 3, this section contains the derivation of the R2035 A/C family, containing the TLAR definition, an advanced conventional technology scenario, and the description of the R2035 PPS.

4.1. R2035 Airframe

Top-Level Aircraft Requirements

The R2035 TLAR are based on the TLAR of the R2000 A/C, while taking into account trends that have a severe impact on them. An example is the change of the boundary conditions for the second climb segment, which were increased to ISA +30 K. This incorporates the impact of global warming and addresses an aspect that already today leads to operational obstructions. Furthermore, noise and emission targets were set in relation to the R2000. The resulting TLAR are shown in Table 6.

Table 6: Top-Level Aircraft Requirements for the CENTRELINE R2035

Parameter	Value
Range and PAX	6500 NM, 340 PAX in 2-class
Take-off field length (MTOM, S-L, ISA)	≤ 2600 m
2nd Climb segment conditions	340 PAX, 100 kg per PAX, DEN, ISA+30 °C
Time-to-climb (1,500 ft to ICA, ISA+10 °C)	≤ 25 mins
Initial cruise altitude (ISA+10 °C)	≥ FL 330
Design cruise Mach number	0.82
Maximum cruise altitude	FL410
Approach speed (MLW, S-L, ISA)	140 KCAS
Landing field length (MLW, ISA)	≤ 2200 m
One engine inoperative altitude (Drift Down)	FL170
Airport compatibility limits	ICAO Code E (52 m < x < 65 m)
Aircraft classification number (flexible,B)	67
External noise & emission target (Reference 2000)	CO_2 -60%; NOx -84%; Noise -11 EPNdb (interpolated SRIA 2035)
Technology freeze – entry into service	2030/2035

Technology scenario

An array of advanced A/C technologies was considered for a potential A/C EIS year 2035. The focus here lied on aerodynamic and structural improvements as well as technologies for sub-systems and power plants. Technological impacts were derived to appropriately reflect target technology readiness level 6 in 2030. In order to establish a consistent technology scenario for the year 2035, and to predict the associated effect on A/C design and performance, a broad survey of aerodynamic, structural and other A/C system technologies was undertaken. Technologies were chosen on account of their probability to enter into service by the year 2035. Their influence on the A/C design was determined by estimations based on data from research and existing A/C data. In the following, feasible technologies, which are included in the airframe design of the R2035 reference A/C in comparison to the R2000 reference A/C, are presented, and an estimation of their impact on A/C performance is given.

The main objective of aerodynamic improvements is the reduction of drag. The selected technologies are tailored to tackle all major shares of A/C drag, such as lift-induced, skin friction, and form drag. The main technological insertions in the field of aerodynamics for the R2035 A/C, therefore, cover an increased aspect ratio wing, Natural Laminar Flow (NLF) nacelles, riblet coatings on the airframe's wetted areas, and an advanced high-lift system.

In order to improve lift-induced drag characteristics, a high aspect ratio wing design is considered. Key enabling technologies include the application of advanced composite materials with improved strength and stiffness properties as well as additive manufacturing techniques [33–35]. Moreover, Gust Load Alleviation (GLA) and Manoeuvre Load Alleviation (MLA) systems, as well as Active Flutter Suppression (AFS) are applied. Here, MLA does not only account for a higher passenger comfort but also counteracts the increased bending moment at the wing root due to the enlarged aspect ratio. To gain significant benefits from MLA, GLA and AFS, systems are needed, which operate analogue to the MLA by individual dynamical oscillations of the control surfaces about the steady-state position to counteract atmospheric turbulence and flutter. The use of the already present control surfaces (ailerons and flaps) as multifunctional movables for MLA, GLA, and AFS induces no change in the structural mass [36–38].

To reduce parasitic drag, riblets technology is applied in the form of a paint coating to passively reduce the local skin friction drag by 8%, leading to a lower zero-lift drag [39, 40]. Riblets are employed on the A/C external surface of an A/C to eliminate cross flow turbulence. For practical reasons, a maximum of 70% of the wetted area can be coated by the riblet film [41]. The riblet coating does not contribute to a higher structural mass, as its mass is in the order of the mass of the paint it replaces. Riblets are assumed to be applied on the fuselage, the wing (without leading edge), as well as the vertical and horizontal stabilizers and the engine nacelles. The engine nacelles are assumed to feature an advanced aerodynamic shaping that provides NLF over 20% of the nacelle chord length. This leads to a decrease of the total drag of each engine nacelle by about 5% [42]. NLF is preferred over a hybrid laminar flow control system as its impact on nacelle structural design, and engine performance is minimal. Thus, no notable mass implications have to be considered.

The influence of each individual aerodynamic technology on the aerodynamic performance (skin friction coefficient and aspect ratio) of the R2035 reference A/C compared to its reference of the year 2000 is summarized in Table 7.

Table 7: Aerodynamic drag reduction R2035 vs. R2000 technology

Component	Parameter	Δ Value rel.	Enabling technologies
Fuselage	Friction drag	- 5.6%	Riblets covering 70% of fuselage wetted area (- 8% local skin friction reduction)
Wing	Friction drag	- 5.6%	Riblets covering 70% of wing wetted area (- 8% local skin friction reduction)
	Aspect ratio	+ 19.0% (AR ≈ 12)	Advanced composite design, improved utilization of composite materials, maneuver and gust load alleviation, active flutter suppression
Empennage	Friction drag	- 5.6%	Riblets covering 70% of empennage wetted area (- 8% local skin friction reduction)
Nacelles	Friction drag	- 10.0%	Riblets covering 70% of nacelle wetted area (- 8% local skin friction reduction), natural laminar flow up to 20% chord length (instead of 5% chord length)

The focus regarding A/C structural technology insertions lies on a mass reduction as a result of the rigorous application of advanced design on all main airframe structural components. This includes an optimized utilization of composite materials together with advanced bonding techniques, as well as improved manufacturing technologies, such as additive manufacturing.

Advanced CFRP are used to replace parts of the R2000 wing made of aluminum, allowing for a R2035 wing, which consists of 90% composite material by mass. The fuselage's main structure is fully made of composite material. The empennage design utilizes advanced composite materials with improved strength and stiffness properties over the year 2000 standard. A geodesic fuselage design in combination with advanced composite materials yields an additional fuselage mass reduction of approximately 10% [43].

In summary, the total structural A/C mass reduction is mainly achieved through the increase of composite materials from 15% to about 70% of total structural mass compared to the R2000 reference A/C as CFRP provides a much better strength-to-weight ratio than metal. Due to advanced numerical technologies, the fiber arrangement can be adapted to the stress distribution. Additional weight savings are achieved through the advanced bonding of composite parts. Rivets and selected fitting metal parts can thus be eliminated. The improvement in strength and stiffness of the used materials, the application of advanced bonding technologies for the composite material, additive manufacturing technologies for non-composite parts, and the application of a geodesic fuselage design also contribute to the overall weight reduction. The influence of the technologies on the mass of the main A/C components is given in Table 8.

Table 8: Structural component mass reduction R2035 vs. R2000 technology

Component	Mass factor	Enabling technologies
Fuselage	- 15%	Fully composite, advanced bonding, advanced composites
	- 10%	Geodetic design
Wing	- 10%	90% composite, advanced materials, and bonding technologies, additive manufacturing, ADHF
Empennage	- 5%	Advanced composite materials and bonding technologies

The mixed hydraulic-pneumatic-electric subsystems of the R2000 A/C are substituted by an all-electrical subsystems architecture, continuing the more-electric A/C design trend already present in the Boeing 787 A/C [44]. The replacement of the fly-by-wire flight control system by a fly-by-light system contributes to a total mass reduction of the control system of 500 kg for the R2035 A/C [45, 46]. Lightweight materials, advanced structure design technologies, as well as additive manufacturing technologies lead to a 20% mass reduction of the cabin furnishing, such as seats, galleys, and inflight entertainment system [47]. The mass impacts of the considered systems technologies for the R2035 reference A/C compared to the year 2000 standard are summarized in Table 9.

Table 9: Systems and equipment mass reduction R2035 vs. R2000 technology

Systems and Equipment	Mass impact	Enabling technologies
Controls System	- 500 kg	Fly-by-light
Furnishing	- 20%	Advanced lightweight material, additive manufacturing

Wing

The wing design of the R2035 A/C was derived from the R2000 A/C. The main change is the increase in wing aspect ratio. The following characteristics define the R2035 wing:

- Planform adjusted for the target aspect ratio of 12
- Thickness distribution identical to R2000
- Twist distribution optimized for constant downwash/elliptical lift
- Airfoils from NASA common research model [48]

The wing's taper ratio is determined as 0.17. Due to the slenderness and high aspect ratio, winglets are not included in the wing design. As for the R2000, a wing loading optimization was conducted, identifying the optimal wing loading for block fuel reduction of the R2035 stretch economic mission. This analysis yielded a wing reference area of 352 m² as an optimum. The aerodynamic performance of the R2035 for mid-cruise is given in Table 10. The effect of the aerodynamic technologies included is reflected in the increase of lift-to-drag ratio compared to the R2000 baseline (see Table 2).

Table 10: R2035 baseline aerodynamics for cruise conditions (FL350, Ma = 0.82, lift coefficient = 0.5)

Parameter	Value [-]
Zero lift drag coefficient	60.8%
Induced drag coefficient	22.4%
Wave drag coefficient	6.8%
Lift-to-drag	21.0

The reduction of induced drag by the increase of aspect ratio is strong. Compared to the induced drag coefficient of the R2000 baseline, a reduction of over 20% was achieved. The overall lift-to-drag increase is moderate (5%) considering the number of technologies that were integrated into the R2035. The main driver is the increase in wetted fuselage area, 10% for the R2035 baseline compared to the R2000 baseline, and the respective increase in friction drag. In addition, the reduced slenderness ratio has to be taken into account, which negatively impacts the form drag of the fuselage.

Fuselage

The design of the R2035 fuselage and cabin is based on the R2000 to provide the same level of comfort. Thus, the seat and aisle width remains mostly unchanged. The cabin configuration is depicted in Figure 9 with a six-abreast layout (2-2-2) in the business class and a nine-abreast (2-5-2) in the economy.

The cabin layout decisions were primarily driven by passenger anthropometrics. An analysis of future passengers was conducted using data of their height and Body Mass Index (BMI) as a proxy for passenger dimensions. The results showed a relatively stable global average passenger height and BMI until 2035. The choice of widening the fuselage to accommodate a nine-abreast baseline configuration for the economy class was motivated by an enhanced flexibility when it comes to the design of a family concept with 375 passengers in the stretched version.

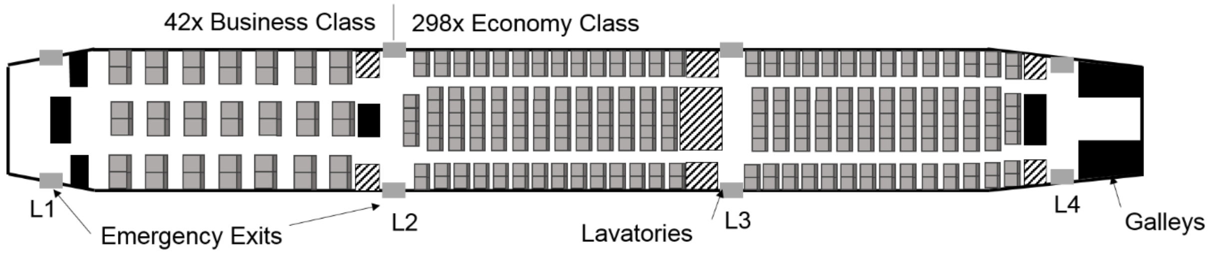

Figure 9: R2035 baseline cabin with 340 PAX in a nine-abreast economy arrangement

The usage of carbon fibers for the fuselage construction allows for the reduction of the wall-thickness, which leads to a reduced fuselage outer diameter keeping the same cabin width [49]. The passenger's perception is positively influenced by the increased headspace, straighter walls, and increased overhead bin storage space. The nine-abreast configuration in a 2-5-2 layout removes the double excuse seat in the middle when the load factor is below 90%. The possibility to use a ten-abreast configuration (3-4-3) in the economy class with a reduced seat width of 17 in would allow airlines to design a high-density cabin. The slightly reduced fuselage length allows for a less constraint fulfillment of the CS/FAR regulations concerning the emergency exits, especially in a stretched family member, as the distance between emergency exit distance shall not be larger than 18.3 m (60 ft) according to Advisory Circular 25.807 [50]. Table 11 presents the main geometric data for the fuselages of the R2035 family.

Table 11: Fuselage data of the R2035 family

Parameter	Shrink	Baseline	Stretch
Passengers [-]	296	340	375
Length [m]	60.2	66.7	71.6
Diameter [m]	6.09	6.09	6.09
Slenderness [-]	9.89	11.0	11.8

Overall Airframe

The structural concept for the wing, fuselage, and empennage of the R2035 was kindly provided by Warsaw University of Technology [51]. The main structural concept of the R2035 wing structure was defined as follows. Two CFRP spars along the whole wingspan, which are strengthened in the pylon suspension area, form the basis of the wing structure. Skin stiffeners (stringers), ribs and skin are also made of CFRP. The percentage of composites is increased to about 90% with respect to mass. Additional weight savings are obtained by using advanced adhesive bonding methods of the composite parts. The fuselage is a "full composite", geodesic structure with a circular cross-section of 6.09 m width in diameter. The primary load-carrying structure is made of CFRP. The internal arrangement is similar to the R2000 A/C. The empennage consists of a classic, fuselage-mounted vertical and horizontal tailplane. Both tailplane structures have an identical composition as in the R2000 A/C. The major structural components of the R2035 A/C are listed in Table 12.

Table 12: R2035 baseline mass breakdown

Component	Mass [t]
Wing	37.1
Fuselage	22.3
Vertical tailplane	1.9
Horizontal tailplane	1.8
Landing gear	10.3
Pylons	2.8
Propulsion system	18.6
Systems	11.8
Furnishing	10.2
Operational items	8.4
Operational empty mass	125.3

The R2035 baseline A/C 3-view is given in Figure 10.

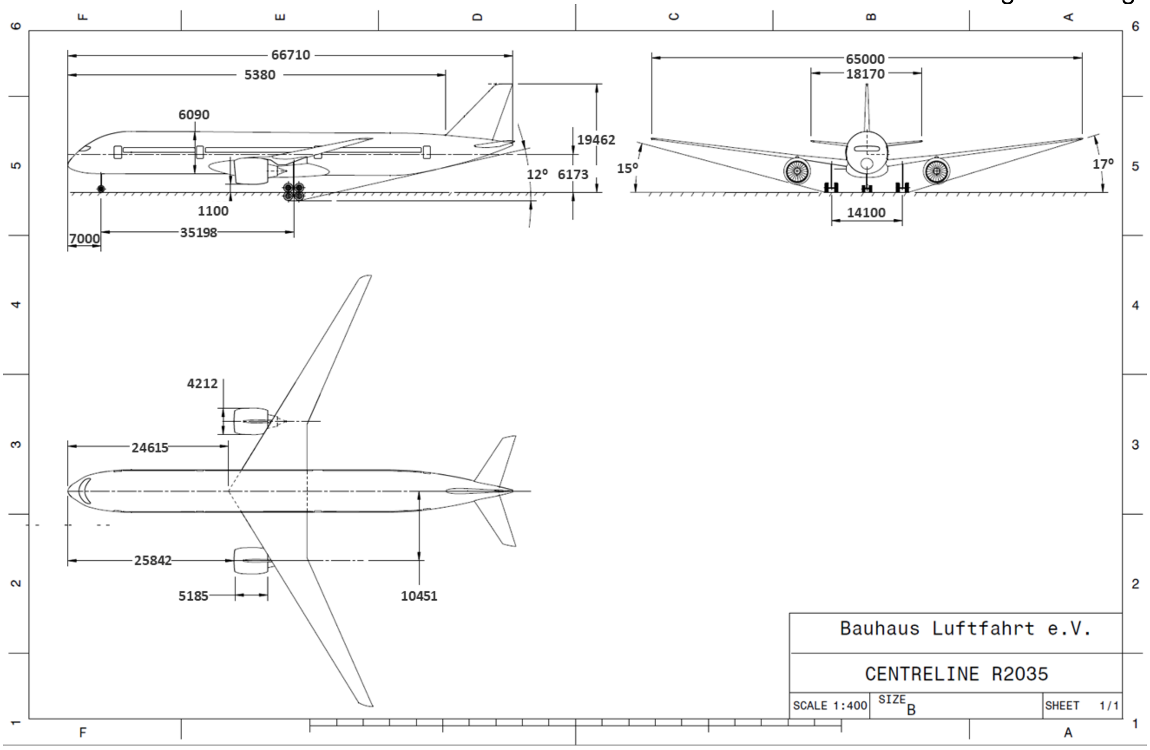

Figure 10: 3-view of the R2035 baseline, dimensions in mm

The R2035 family members are shown in Figure 11, with the shrink at the top, the baseline in the middle and the stretch at the bottom of the figure.

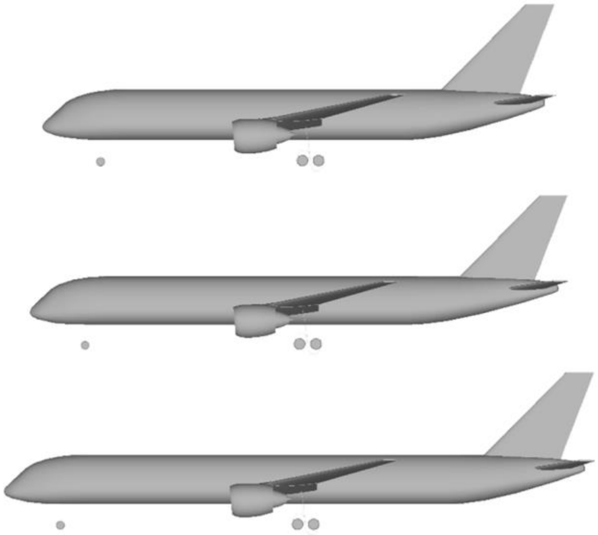

Figure 11: R2035 aircraft family

4.2. 2035 power plant

The R2035 A/C is equipped with geared turbofans featuring Ultra-High Bypass Ratio (UHBR) in excess of 16. Best and balanced cycle settings, including temperature and pressure levels, were selected based on conceptual cycle studies. Models for the prediction of component design efficiencies and pressure losses were adjusted to reflect the advanced technology status. With the intention to counteract the weight and external drag penalties associated with the large propulsor dimensions intrinsic to UHBR, a slim and short nacelle design was envisioned with the inner intake contour featuring advanced acoustic liners for noise suppression. Further advanced design elements include an integrated fan stator and strut, brush seals [52] as well as a variable area fan nozzle, thus improving fan operability for the targeted low specific thrust design.
For the potential year 2035 EIS scenario, a set of technological features was considered to be incorporated in the R2035 power plants. Beyond the rigorous application of 3D aerodynamic design, turbo components are considered to feature aspects such as advanced clearance control and endwall contouring [53], casing treatments [54], and active surge control. Advanced cooling technologies, including dimple [55] and effusive cooling techniques [56], are considered to contribute to reduced cooling air demands. The application of enhanced material options is considered to allow for elevated temperature levels relative to the R2000 power plant while offering mass savings. Apart from excessive use of CFRP in the low-temperature regime (e.g., the fan assembly), titanium metal matrix composites [57], titanium-aluminides [58], and ceramic matrix composites [58] are seen as potential options. In addition, advanced manufacturing techniques, including large-scale utilization of additive layer manufacturing for elements such as liners, fuel nozzles, casings, and potentially even blades and vanes [59], are promising candidates for realizing significant mass savings and possibly lifespan improvements [58].
The cycle design and performance modeling for the R2035 PPS is discussed in more detail by Bijewitz et al. [60]. The PPS mass assessment was conducted by Chalmers University of Technology [61]. Flow path sizing was conducted at the top of climb (FL350, Ma = 0.82, and ISA +10 K) conditions were taken into account during sizing. Table 13 lists key data for the R2035 PPS.

Table 13: R2035 power plant system key data

Parameter	Value
Fan diameter	3.36 m
Nacelle diameter	4.21 m
Nacelle length	5.19 m
Design bypass ratio	16.4*
Nominal Take-Off Thrust (SLS, ISA+0 K)	377 kN
Thrust specific fuel consumption (mid-cruise @FL370, Ma = 0.82, 46.7 kN)	14.0 [g/s/kN]

*Flow path sizing point at top-of-climb (Ma = 0.82, FL350, ISA+10 K)

4.3. R2035 mission performance and R2000 comparison

Similar to the R2000 family, the R2035 family was implemented in APD. The outcome of the overall A/C assessment, including snowball effects of mass data, aerodynamic analysis and mission performance calculations yielded results for all members of the two A/C families. The resulting data and their comparison towards the R2000 family are shown in Table 14.

Table 14: Result comparison of the R2000 family with the R2035 family

Parameters values in [t]	R2000 shrink	R2035 shrink	Δ%	R2000 base	R2035 base	Δ%	R2000 stretch	R2035 stretch	Δ%
Design mission block fuel	92.8	61.7	-33.5	**98.0**	**65.5**	**-33.2**	102.7	68.4	-33.4
Operation Empty Mass	147.1	121.0	-17.7	**152.1**	**125.3**	**-17.6**	157.2	128.8	-18.1
Maximum Take-off Mass	278.3	222.4	-20.1	**293.2**	**235.1**	**-19.8**	306.9	245.2	-20.1

The baseline members of both families will be used for the integration of the propulsive fuselage technology. The R2035 baseline states a solid and competitive foundation for a fair assessment of the PFC introduction with an EIS in 2035.

5. CONCLUSION

The results from the application scenario and reference A/C definition performed as part of the CENTRELINE project were presented.
An analysis of the air traffic demands and A/C market segment trends for a target propulsive fuselage A/C EIS year 2035 was conducted. The market forecast showed a very strong influence on the intercontinental traffic between Europe and Asia. The biggest potential was identified for a design mission with 340 passengers and 6500 NM range. The results were discussed, and in collaboration between Airbus and BHL, a consensus was reached to set this design mission as the target, thereby defining the target application for the CENTRELINE research and innovation actions.
A suitable set of TLAR was compiled based on an existing A/C design with the best possible data availability and similarity concerning the design mission. This A/C was determined to be the Airbus A330-300 equipped with Rolls-Royce Trent 700 series power plants. Based on the A330-300, an airframe and propulsion system was designed and incorporated into a family concept. The resulting configuration represents a suitable year 2000 reference A/C (R2000) appropriate for SRIA benchmarking purposes.
For a representative technology level for a 2035 EIS, a multi-disciplinary scenario of advanced technologies including power plant, systems, structures, aerodynamics, and annexed technologies was established in cooperation between BHL, Airbus, and Warsaw University of Technology, forming the basis for the year 2035 reference A/C (R2035) definition. These technologies were integrated into the conceptual A/C design tool APD, and an optimized R2035 was derived. The advanced year 2035 GTF propulsion system was developed by BHL and Chalmers University of Technology. Expert advice provided by MTU Aero Engines AG was used to set up a realistic technology scenario for the year 2035 power plant. Cycle studies were conducted to determine best and balanced key cycle properties and design and performance decks created for subsequent evaluation at A/C level. The specification of the fuselage structural concept for the R2035 was developed by Warsaw University of Technology. In cooperation between Warsaw University of Technology and BHL, CAD models for the sized R2000 and R2035 reference A/C were created, representing the geometry of the outer mold line.
The R2000 and R2035 were designed as a baseline of an A/C family, including a common design for main structural components sized for the critical member of the family. The family concepts contain the baseline and deducted stretched and shrinked versions. The implications on the performance on the baseline, e.g., sizing of the engine for the stretched family member, were included in the baseline and taken into account for its performance assessment. The R2035 baseline design has a block fuel reduction for the design mission of 33% compared to the R2000 baseline.
The designed A/C served as the basis for the derivation of the PFC A/C, as the data source for the CENTRELINE partners, and as the reference for comparison and assessment. The results of the PFC performance assessment are documented in the dedicated CENTRELINE deliverable 2.11 and a journal paper [62, 63].

6. ACKNOWLEDGEMENTS

The authors convey their gratitude to the CENTRELINE members of Airbus, Chalmers University of Technology, Delft University of Technology and Warsaw University of Technology, and Michael Schmidt for their support and input during the creation of the reference A/C and propulsion system. The CENTRELINE project has received funding from the European Union's Horizon 2020 research and innovation program under Grant Agreement No. 723242.

REFERENCES

[1] A. Seitz *et al.,* "Concept Validation Study for Fuselage Wakefilling Propulsion Integration," in *31st Congress of the International Council of the Aeronautical Sciences*, Belo Horizonte, Brazil, 2018. [Online]. Available: https://www.icas.org/ICAS_ARCHIVE/ICAS2018/data/papers/ICAS2018_0342_paper.pdf

[2] ACARE, "Strategic research & innovation agenda - 2017 update," advisory Council for aviation research and innovation in europe, 2017. [Online]. Available: https://www.acare4europe.org/sites/acare4europe.org/files/document/ACARE-Strategic-Research-Innovation-Volume-1.pdf

[3] H. J. Steiner, A. Seitz, K. Wieczorek, K. Plötner, A. T. Isikveren, and M. Hornung, "Multi-disciplinary design and feasibility study of distributed propulsion systems," in *28th Congress of the International Council of the Aeronautical Sciences*, Brisbane, Australia, 2012. [Online]. Available: http://www.scopus.com/inward/record.url?eid=2-s2.0-84878529161&partnerID=tZOtx3y1

[4] ICAO, *Facts and Figures.* [Online]. Available: https://www.icao.int/sustainability/Pages/Facts-Figures_WorldEconomyData.aspx

[5] A. T. Isikveren *et al.,* "Distributed propulsion and ultra-high by-pass rotor study at aircraft level," *The Aeronautical Journal*, vol. 119, no.

1221, pp. 1327–1376, 2015, doi: 10.1017/S0001924000011295.
[6] AIRBUS S.A.S, *Global Market Forecast 2012 - 2031: Navigating the Future*.
[7] Boeing, *Current Market Outlook 2012-2031.* [Online]. Available: https://www.boeing.com/commercial/market/commercial-market-outlook/
[8] ICAO, "Environmental Report 2010," 2010. Accessed: Sep. 23 2019. [Online]. Available: https://www.icao.int/environmental-protection/Documents/Publications/ENV_Report_2010.pdf
[9] N. Teyssier, "ACI Airport Statistics and Forecasting Workshop – Aviation Statistics & Data: A Vital Tool for the Decision Making Process," 2012.
[10] N. Teyssier, "Global Air Transport Outlook," in *37th Annual FAA Aviation Forecast Conference*, Washington, D.C., 2012.
[11] ICAO, *Outlook for Air Transport to the Year 2025.* [Online]. Available: https://www.icao.int/sustainability/Documents/C313_Outlook_En.pdf
[12] Rolls Royce, "Market Outlook 2009 – Forecast 2009-2028," 2009.
[13] ACI, "Global Traffic Forecast 2008-2027," Airport Council International, 2009.
[14] K. Ward, *The World in 2050: From the Top 30 to the Top 100.* [Online]. Available: https://big.assets.huffingtonpost.com/world2050.pdf (accessed: Sep. 23 2019).
[15] K. O. Ploetner and M. Schmidt, "Forecast Summary," Internal Report 13008, 2013.
[16] AIRBUS S.A.S, *Airbus Global Market Forecast growing horizon 2017-2036.* [Online]. Available: http://www.airbus.com/content/dam/corporate-topics/publications/backgrounders/Airbus_Global_Market_Forecast_2017-2036_Growing_Horizons_full_book.pdf
[17] Boeing, *Market Outlook 2017-2036.* [Online]. Available: http://www.boeing.com/resources/boeingdotcom/commercial/market/current-market-outlook-2017/assets/downloads/2017-cmo-6-19.pdf
[18] UAC, *Market Outlook 2017-2036.* [Online]. Available: https://uacrussia.ru/upload/iblock/745/7456e24c203303343f959617195620a3.pdf
[19] OAG Official Airline Guide, "Scheduled flight data 2012," 2012.
[20] AIRBUS S.A.S, *A330 AutoCAD 3-View Aircraft Drawings.* [Online]. Available: http://www.aircraft.airbus.com/support-services/airport-operations/autocad-3-view-aircraft-drawings/ (accessed: Sep. 1 2017).
[21] AIRBUS S.A.S, *A330 Aircraft Characteristics Airport and Maintenance Planning.* [Online]. Available: https://www.airbus.com/content/dam/corporate-topics/publications/backgrounders/techdata/aircraft_characteristics/Airbus-Commercial-Aircraft-AC-A330.pdf
[22] E. Obert, *Aerodynamic Design of Transport Aircraft*. Amsterdam: IOS Press, 2009.
[23] C. D. Harris, "NASA supercritical airfoils: A matrix of family-related airfoils," NASA Langley Research Center, Hampton, VA, United States, Washington, United States, Technical Report NASA-TP-2969, 1990. [Online]. Available: https://ntrs.nasa.gov/search.jsp?R=19900007394
[24] A. Tovey, "Rolls-Royce boosted by £1.4bn order for troubled Trent 700 engines," *The Telegraph*, 2015. [Online]. Available: https://www.telegraph.co.uk/finance/11750406/Rolls-Royce-wins-two-new-contracts-worth-2.2bn.html
[25] *RB211 Trent 700 series engines: Type-Certificate Data Sheet*, EASA.E.042, European Union Aviation Safety Agency (EASA), Feb. 2019. [Online]. Available: https://www.easa.europa.eu/sites/default/files/dfu/EASA%20E%20042%20TCDS%20issue%2005.pdf
[26] M. Daly, *Jane's aero engines 2013/2014,* 2nd ed. Coulsdon: IHS, 2013.
[27] S. Kaiser, A. Seitz, S. Donnerhack, and A. Lundbladh, "Composite Cycle Engine Concept with Hectopressure Ratio," *Journal of Propulsion and Power*, vol. 32, no. 6, pp. 1413–1421, 2016, doi: 10.2514/1.B35976.
[28] J. Bijewitz, A. Seitz, and M. Hornung, "Extended Design Studies for a Mechanically Driven Propulsive Fuselage Aircraft Concept," in *2018 AIAA Aerospace Sciences Meeting*, Kissimmee, Florida, 2018.
[29] A. Seitz, M. Nickl, A. Stroh, and P. C. Vratny, "Conceptual study of a mechanically integrated parallel hybrid electric turbofan," *Proceedings of the Institution of Mechanical Engineers, Part G: Journal of Aerospace Engineering*, vol. 232, no. 14, pp. 2688–2712, 2018, doi: 10.1177/0954410018790141.
[30] J. Kurzke, "GasTurb 12 - Design and Off-Design Performance of Gas Turbines," Germany, 2013. Accessed: Mar. 2 2019. [Online]. Available: http://www.gasturb.de/Gtb12Manual/GasTurb12.pdf
[31] *Type Certificate Data Sheet E39NE, Rolls-Royce plc RB211 Trent 700 series*, TCDS No.: E.042, European Aviation Safety Agency, Dec. 2019.
[32] TXT, *Pacelab APD.* [Online]. Available: https://www.txtgroup.com/markets/solutions/pacelab-apd/
[33] D. Hayes, M. M. Lone, J. Whidborne, and E. Coetzee, "Evaluating the Rationale for Folding Wing Tips Comparing the Exergy and Breguet Approaches," in *55th AIAA Aerospace Sciences Meeting*, Grapevine, Texas, 2017, p. 1.

[34] G. Kennedy and J. Martins, "A Comparison of Metallic and Composite Aircraft Wings Using Aerostructural Design Optimization," in *Aviation Technology, Integration, and Operations (ATIO) Conferences: 12th AIAA Aviation Technology, Integration, and Operations (ATIO) Conference and 14th AIAA/ISSMO Multidisciplinary Analysis and Optimization Conference*, Indianapolis, Indiana, 2012, p. 1.
[35] J. Martins, G. Kennedy, and G. K. Kenway, "High Aspect Ratio Wing Design: Optimal Aerostructural Tradeoffs for the Next Generation of Materials," in *52nd Aerospace Sciences Meeting, 13-17 January 2014,National Harbor, Maryland*, National Harbor, Maryland, 2014, p. 587.
[36] B. K. Stanford, "Optimization of an Aeroservoelastic Wing with Distributed Multiple Control Surfaces," *Journal of Aircraft*, vol. 53, no. 4, pp. 1131–1144, 2016, doi: 10.2514/1.C033613.
[37] J. Xu and I. Kroo, "Aircraft Design with Maneuver and Gust Load Alleviation," in *29th AIAA Applied Aerodynamics Conference*, Honolulu, Hawaii, 2011, p. 131.
[38] J. Xu, "Aircraft design with active load alleviation and natural laminar flow,"
[39] J. Reneaux, "Overview on drag reduction technologies for civil transport aircraft," in *European Congress on Computational Methods in Applied Sciences and Engineering*, Jyväskylä, 2004.
[40] S. Sayad Saravi and K. Cheng, "A review of drag reduction by riblets and micro-textures in the turbulent boundary layers," *European Scientific Journal*, 2013, pp. 62–81, 2013.
[41] D. W. Bechert, M. Bruse, W. Hage, and R. Meyer, "Fluid mechanics of biological surfaces and their technological application," *Die Naturwissenschaften*, vol. 87, no. 4, pp. 157–171, 2000, doi: 10.1007/s001140050696.
[42] S. Li and Y. Zhong, "A Turbofan-Engine Nacelle Shape Design and Optimization Method for Natural Laminar Flow Control," in *Volume 1: Aircraft Engine; Fans and Blowers; Marine*, Seoul, South Korea, 2016.
[43] C. Hühne, "Final Report Summary – ALaSCA (Advanced Lattice Structures for Composite Airframes)," 2014.
[44] L. Faleiro, "Beyond the More Electric Aircraft," *Aerospace America*, pp. 35–40.
[45] G. T. Seng, "Overview of NASA Research in Fiber Optics for Aircraft Controls," NASA Technical Memorandum 100919, 1988.
[46] J. R. Todd, J. A. Hay, and T. Dinh, "Integrating Fly-By-Light/Power-By-Wire Flight Control Systems on Transport Aircraft," in *AIAA IEEE Digital Avionics Systems Conference: 12th DASC*, 1993, pp. 457–462.
[47] G. Norris, "Boeing plans plain grey natural laminar flow nacelles for 787s in bid to reduce fuel burn," *Flight Global*, 2006. [Online]. Available: https://www.flightglobal.com/news/articles/picture-boeing-plans-plain-grey-natural-laminar-flo-207769/
[48] J. Vassberg, M. Dehaan, M. Rivers, and R. Wahls, "Development of a Common Research Model for Applied CFD Validation Studies," in *26th AIAA Applied Aerodynamics Conference*, Honolulu, Hawaii, 2008, 6--9. [Online]. Available: https://ntrs.nasa.gov/search.jsp?R=20080034653
[49] J. M. McClellan and D. Simanaitis, "Carbon Fiber Flyers," *Flying Magazine*, Band 132, Nr. 7, pp. 45–58, 2005.
[50] *AC 25.807-1 - Uniform Distribution of Exits,* Federal Aviation Administration, Aug. 1990. [Online]. Available: https://www.faa.gov/documentLibrary/media/Advisory_Circular/AC_25_807-1.pdf
[51] Z. Goraj, B. Goliszek, M. Kowalski, A. Seitz, F. Peter, and F. Meller, "Strategy and Implementation of a Parametric CAD Model for R2035 Aircraft Structure and External Configuration," in *31st Congress of the International Council of the Aeronautical Sciences*, Belo Horizonte, Brazil, 2018. [Online]. Available: http://www.icas.org/ICAS_ARCHIVE/ICAS2018/data/papers/ICAS2018_0752_paper.pdf
[52] B. Outirba and P. Hendricks, "Experimental Testing of Carbon Brush Seals for Oil Mist Applications in Modern Aero-Engines," *NATO MP AVT-230-11*, 2015.
[53] C. Dorfner, A. Hergt, E. Nicke, and R. Moenig, "Advanced Nonaxisymmetric Endwall Contouring for Axial Compressors by Generating an Aerodynamic Separator—Part I: Principal Cascade Design and Compressor Application," *Journal of Turbomachinery*, vol. 133, no. 2, p. 21026, 2011, doi: 10.1115/1.4001223.
[54] G. A. Brignole, "Parameter zur Auslegung effizienter Gehäusestrukturierungen," Dissertation, Institut für Luft- und Raumfahrt, Lehrstuhl für Flugantriebe, Technische Universität München, Munich, 2010. [Online]. Available: https://mediatum.ub.tum.de/doc/823172/823172.pdf
[55] R. S. Bunker and K. F. Donnellan, "Heat Transfer and Friction Factors for Flows Inside Circular Tubes With Concavity Surfaces," *Journal of Turbomachinery*, vol. 125, no. 4, pp. 665–672, 2003, doi: 10.1115/1.1622713.
[56] G. Cerri, A. Giovannelli, L. Battisti, and R. Fedrizzi, "Advances in effusive cooling techniques of gas turbines," *Applied Thermal Engineering*, vol. 27, no. 4, pp. 692–698, 2007, doi: 10.1016/j.applthermaleng.2006.10.012.

[57] International Air Transport Association (IATA), *IATA Technology Roadmap: Technical Annex.* [Online]. Available: https://www.iata.org/whatwedo/environment/Documents/technology-roadmap-annex.pdf
[58] D. Carlson, “GE Aviation: Perspectives on Clean, Efficient Engines: Presentation,” May. 2013.
[59] General Electric, “Additive Manufacturing – Present and Future: Presentation at Manufacturing First Expo and Conference,” Green Bay, WI, Oct. 2014.
[60] J. Bijewitz, A. Seitz, and M. Hornung, “Power Plant Pre-Design Exploration for a Turbo-Electric Propulsive Fuselage Concept,” in *Joint Propulsion Conference*, Cincinnati, Ohio, 2018.
[61] S. Samuelsson, P. Olivier, R. Merkler, and G. Wortmann, “Adaption of a turbofan engine for high power offtakes for a turbo-electric propulsive fuselage concept,” in *24th International Society of Air-breathing Engines (ISABE) Conference*, Canberra, Australia, 2019.
[62] A. Seitz *et al.,* “Proof of Concept Study for Fuselage Boundary Layer Ingesting Propulsion,” *Aerospace Journal*, 2020, doi: 10.3390/aerospace8010016.
[63] A. Habermann *et al.,* “D2.11 - Summary report on multi-disciplinary design results: Deliverable 2.11 of the EU project CENTRELINE (ConcEpt validatioN sTudy foR fusElage wake-filLIng propulsioN),” 2020.